Nanoscale stiffness of individual dendritic molecules and their aggregates

Vladimir V. Tsukruk,[a] Hennady Shulha, and Xiaowen Zhai
Department of Materials Science & Engineering, Iowa State University, Ames, Iowa 50011

(Received 16 September 2002; accepted 11 December 2002)

We demonstrate that carefully designed micromapping of the surface stiffness with nanoscale resolution could reveal quantitative data on the elastic properties of compliant, dendritic organic molecules with nanoparticulate dimensions below 3 nm. Much higher elastic modulus was observed for individual, fourth generation dendritic molecules due to their more shape persistent conformation. Large, reversible, elastic deformation is a distinct characteristic of the nanomechanical response observed for individual dendritic molecules. Such a ''rubbery'' response could be an indication of spatial constraints imposed on vitrification of dendritic molecules tethered to the functionalized interface. Surprisingly, an increased stiffness was also found for the third generation dendritic molecules within long aggregates. © *2003 American Institute of Physics.*
[DOI: 10.1063/1.1544056]

An understanding of the nanomechanical properties of individual organic and polymeric molecules, and their molecular aggregates at solid surfaces, is critical for the design of electromechanical and fluidic nanodevices with nanoscale contact interactions.[1,2] Direct measurements of elastic properties of individual organic molecules is possible only with atomic force microscopy (AFM). However, current studies are mainly limited to qualitative visualization of the surface stiffness distribution and polymer films.[3] An AFM-based pull-off mode is frequently applied to conduct analysis of tensile properties of long-chain molecules and the strength of binding interactions.[4]

In this letter, we report the surface stiffness of individual nanoparticulate molecules, as well as their surface clusters (aggregates) containing a limited number of molecules. Stiffness is measured in an AFM compression mode by using surface micromapping.[5] We choose dendritic molecules, namely, hyperbranched polyesters, which are known for forming compliant nanoparticles with a diameter of several nanometers,[6–9] as an example of molecules in which nanomechanical properties cannot be tested with tensile-mode AFM. The internal architecture of these molecules may be represented as a highly branched, tree-like structure containing a central core, branches, a certain level of internal defects, and a high concentration of terminal functional groups.[10,11] These molecules represent a new class of functionalized materials with promising interfacial nanoscale properties.[12–14]

We study third (G3)- and fourth (G4)-generation dendritic molecules (hyperbranched polyesters with molecular weight of approximately 3000 to 7000, respectively, see Fig. 1 for chemical formulas). These molecules possess slightly flattened and spherical conformations on solid substrates with diameter of 2 and 3 nm, respectively, as we demonstrated earlier.[15] To get reliable quantification of the nanomechancial properties, the micromapping of the surface stiffness was carefully designed as follows. To enhance the surface stability of the molecular aggregates and provide an ideal landscape for the tip-molecule interactions, the dendritic molecules were anchored to an atomically flat silicon wafer surface via chemical attachment to an amine-terminated self-assembled monolayer (SAM) from 3-aminopropyltriethoxysilane fabricated according to the known routine.[16,17] As was demonstrated earlier and was tested in current studies as well, silicon surface carefully modified this way is terminated with a 0.6-nm-thick monolayer with the microroughness below 0.2 nm and high concentration of amine groups, which could serve for anchoring of hyperbranched molecules with hydroxyl terminal groups.

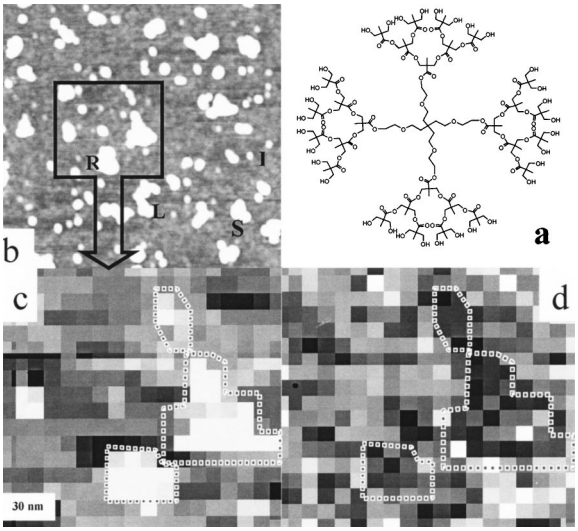

FIG. 1. Chemical formula of third generation hyperbranched molecules in extended idealized configuration (a). Tapping AFM image ($750\times750\times10$ nm) of anchored G3 dendritic molecules and their aggregates (b); examples of different aggregates are marked as follows: I-individual molecule, R-round aggregate, and S-short aggregate, L-long aggregate. The 16×16 micromapping of G3 aggregates from surface area selected in the image in Fig. 1(b): topographical map of the surface area with three different aggregates marked with dotted lines [(c), lighter color means higher elevation] and corresponding distribution of surface stiffness [(d), darker color means lower stiffness]; a variation of data in a single pixel is caused by nanoscale mechanical instabilities and thermal drifts that could compromise an individual measurement.

[a]Author to whom correspondence should be addressed; electronic mail: vladimir@iastate.edu

Anchored molecules are able to resist high stresses introduced by the AFM tip unlike physisorbed molecules, which could easily escape from the contact area. In addition, to reduce the adhesive forces, the AFM tips were chemically modified with a methyl-terminated octadecyltrichlorosilane SAM according to the established routine.[18] This way, a silicon oxide surface is coated with a 2.5 nm film of the hydrophobic SAM with nonpolar terminal groups that tremendously reduces the capillary forces acting between the modified AFM tip and substrate. Considering that the elastic modulus of this layer (from 1 to 5 GPa for similar alkyl monolayers[19–21]) is significantly (3–10 times) higher than the elastic modulus of the dendritic molecules, the presence of this layer does not affect measurements.

Surface nanoprobing was conducted in a force-volume mode[22] with pixel-to-pixel distances of 3–12 nm and local deformation not exceeding 2–4 nm to avoid irreversible compression of the compliant molecules.[23] The tip deflection, Δz_{defl}, during the compression cycle was measured at each location and converted to a load-indentation curve. These data were analyzed using Sneddon's or Hertzian contact mechanics combined with a double-spring, variable constant model as was described in detail elsewhere.[24,25] Briefly, the initial Sneddon equations for a parabolic indenter[26–28] were adapted for the AFM probing in the form

$$E = \frac{3(1-\nu^2)}{8\sqrt{2R}} kn \frac{\Delta z_{\mathrm{defl},i,i-1}}{\sqrt{h}i\Delta h_{i,i-1}},$$

where i, $i-1$ refers to the adjacent tip displacements, h_i is current displacement, and $\Delta h_{i,i-1}$ is an increment, k_n is a spring constant of the tip. The composite tip radius is given by R where $1/R^2 = 1/R_{\mathrm{tip}}^2 + 1/R_{\mathrm{surf}}^2$ and E is the composite modulus $1/E = (1-\nu_1^2)/E_1 + (1-\nu_2^2)/E_2$ with R_{tip}, E_1, ν_1 and R_{surf}, E_2, ν_2 being the radii, Young's moduli, and the Poisson ratios for the AFM tip and molecules, respectively. Appropriate values were taken for the silicon and the dendritic molecules.

In order to quantify the experimental AFM data, we measured the normal spring constants of the tip (within 1–5 N/m) according to added mass and spring-against-spring techniques.[29] By imaging reference samples of 5-nm-diam gold nanoparticles, the tip end shape was approximated by a parabolic function to deduce effective tip radii (within 10–20 nm). The radius of the contact area estimated with the Hertzian model was within 1–2 nm, which is close to the dimensions of the molecules and verifies the tip-single molecule contact. Finally, the tip velocity varied from 10 to 40 nm/s to assure that the viscous contribution was insignificant. Zoom-out scanning was conducted after the surface micromapping to assure reversible deformation and to optimize a threshold tip deflection. All measurements were conducted on Dimension and Multimode Nanoscope IIIa microscopes. For surface micromapping, we selected surface areas from 200 $\times$200 nm to 1×1 μm across and collected arrays of up to 64×64 force-distance curves. Selected surface areas contained at least several clusters of different dimensions. Despite random local variations due to a noise contribution for nanometer displacements, a clear correlation can be seen between locations and shapes of molecular clusters on the high-resolution AFM image, and the corresponding topographical and elastic surface maps (Fig. 1).

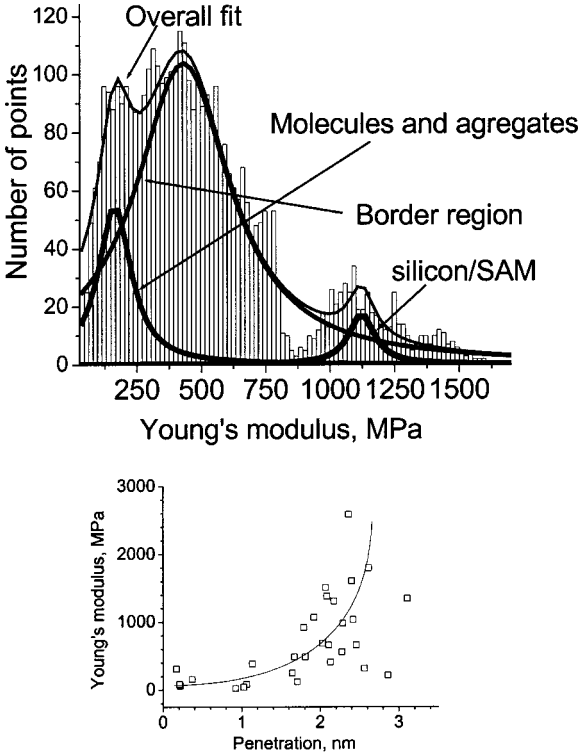

FIG. 2. Overall statistics of elastic moduli collected from 1×1 μm surface area showing three different levels of the stiffness for aggregates, aggregate edges, and modified silicon (top); an example of an elastic modulus depth profile for four different G3 dendritic molecules showing a sharp rise of "apparent" stiffness for high degrees of compression due to the presence of the underlying silicon surface; the line is a guide for the eye (bottom).

G3 dendritic molecules formed a variety of surface aggregates and displayed partial bilayer formation (Fig. 1, see discussion and comparison G3 and G4 molecules in Ref. 15). The number of molecules within these aggregates evaluated from molecular dimensions after correction for tip convolution, ranged from 3 to 40. We observed a coexistence of individual molecules, small round aggregates, as well as short-chain and long-chain aggregates (Fig. 1). Raw force-distance curves collected for individual molecules display typical characteristics for compliant objects on a stiff solid substrate: initial jump into contact (deformation usually did not exceed 0.5 nm) was followed by a compliant region with low resistance for the next 2–3 nm and, finally, deflection becomes linear with a slope close to 1 indicating an intimate contact with a stiff solid surface (not shown).[23] The corresponding depth profiling of the elastic response shows a virtually constant level of the elastic modulus for 1.5–2 nm of initial deformation, followed by a sharp increase due to the compression against the stiff silicon substrate (Fig. 2).[21,23]

Statistical analysis of the surface distribution of the molecular stiffness under small deformations clearly demonstrated the presence of three distinctive stiffness levels for surfaces covered with dendritic molecules (Fig. 1). On the corresponding histogram distribution, high elastic modulus of >1.1 GPa was obtained for the surface areas of the SAM-modified silicon surface (Fig. 2). A broad maximum at lower values of the elastic modulus histogram was composed of two peaks, which corresponded to the central areas of the

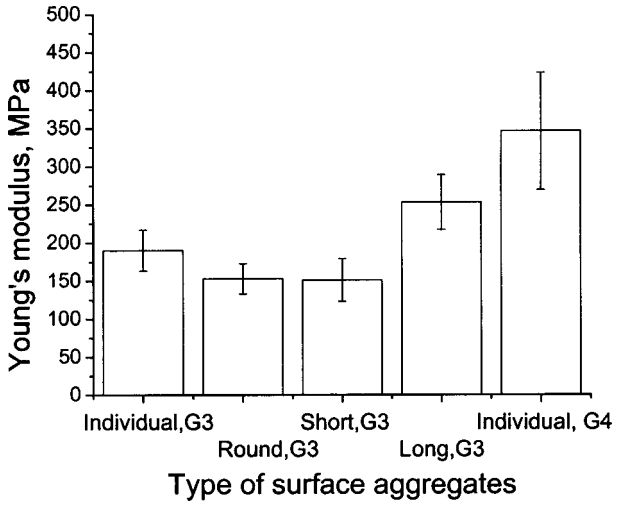

FIG. 3. The values of elastic moduli obtained for different types of surface aggregates from G3 and G4 dendritic molecules (top).

aggregates and the aggregate borders. The absolute values of the elastic modulus for the molecules within internal aggregate regions were within 100–300 MPa (Fig. 2). The border regions showed overestimated elastic modulus values due to the lateral physical contact of the AFM tip with the aggregate edges.

To evaluate the elastic properties of individual dendritic molecules and aggregates of different dimensions, we conducted pixel-by-pixel analysis of different aggregates excluding the aggregate edges. As a result, we grouped all data in four different classes: individual molecules, round aggregates, short (number of molecules below 10) and long aggregates (Fig. 3). The elastic modulus of individual G3 molecules was determined to be 190 ± 30 MPa. This value is characteristic of flexible macromolecules above the glass transition temperature. A high level of reversible, elastic deformation (up to 60% of compression) is another characteristic of the nanomechanical response observed for individual dendritic molecules. Considering that the nominal glass transition temperature for these materials in the bulk state is 80 °C, such a ''rubbery'' response could be an indication of spatial constraints imposed on vitrification of dendritic molecules tethered to the functionalized interface. The phenomenon of significant lowering of the glass transition temperature has been observed for macromolecules confined onto interfaces.[30]

The value of the elastic modulus remains virtually unchanged for small aggregates (150 ± 25 MPa). Surprisingly, the dendritic molecules aggregated in long aggregates are much stiffer with the elastic modulus reaching 250 ± 30 MPa (Fig. 3). The increased molecular stiffness of the dendritic molecules aggregated in long clusters remains to be understood. Finally, higher generation G4 dendritic molecules possess a much higher elastic modulus approaching 350 ± 70 MPa (Fig. 3). This reflects a higher molecular stiffness of the dendritic molecules of higher generation with more congested shells containing 64 terminal branches.

The authors thank S. Peleshanko for technical assistance. Funding from the National Science Foundation, Grant Nos. DMR-0074241 and CMS-0099868, is gratefully acknowledged.

[1] H. G. Graighead, Science **290**, 1532 (2000).
[2] B. Bhushan, J. N. Israelachvili, and U. Landman, Nature (London) **374**, 607 (1995).
[3] M. Schneider, M. Zhu, G. Papastavrou, S. Akari, and H. Mohwald, Langmuir **18**, 602 (2002); R. Overney, V. V. Tsukruk, in *Scanning Probe Microscopy of Polymers*, edited by B. Ratner and V. V. Tsukruk, ACS Symposium Series (American Chemical Society, Washington, DC, 1998), Vol. 694, p. 2.
[4] E.-L. Florin, V. T. Moy, and H. E. Gaub, Science **264**, 415 (1994).
[5] Nanoscope III, Digital Instruments, Santa Barbara, CA, 1995.
[6] *Dendritic Molecules*, edited by G. R. Newkome, C. N. Moorefield, and F. Vogtle (VCH, Weinheim, 1996).
[7] V. V. Tsukruk, Adv. Mater. **10**, 253 (1998).
[8] J. Li, L. T. Piehler, D. Qin, J. R. Baker, Jr., and D. A. Tomalia, Langmuir **16**, 5613 (2000).
[9] D. A. Tomalia and J. M. J. Frechet, J. Polym. Sci. A **40**, 2719 (2002).
[10] B. Voit, J. Polym. Sci., Part A: Polym. Chem. **38**, 2505 (2000).
[11] R. Mezzenga, L. Boogh, J.-A. E. Manson, and B. Pettersson, Macromolecules **33**, 4373 (2000).
[12] D. C. Tully and M. J. Frechet, Chem. Commun. (Cambridge) **14**, 1229 (2001).
[13] S. Sheiko and M. Moller, Top. Curr. Chem. **212**, 137 (2001).
[14] *Dendrimers and Other Dendritic Polymers*, edited by J. M. J. Fréchet and D. A. Tomalia (Wiley, New York, 2002).
[15] A. Sidorenko, X. W. Zhai, S. Peleshanko, A. Greco, V. V. Shevchenko, and V. V. Tsukruk, Langmuir **17**, 5924 (2001).
[16] V. V. Tsukruk, Adv. Mater. **13**, 95 (2001).
[17] A. Noy, D. V. Vezenov, and C. M. Lieber, Annu. Rev. Mater. Sci. **27**, 381 (1997).
[18] V. V. Tsukruk and V. N. Bliznyuk, Langmuir **14**, 446 (1998).
[19] T. P. Weihs, Z. Nawaz, S. P. Jarvis, and J. B. Pethica, Appl. Phys. Lett. **59**, 3536 (1991).
[20] V. V. Tsukruk, V. N. Bliznyuk, J. Hazel, D. Visser, and M. P. Everson, Langmuir **12**, 4840 (1996).
[21] V. V. Tsukruk, H.-S. Ahn, A. Sidorenko, and D. Kim, Appl. Phys. Lett. **80**, 4825 (2002).
[22] V. V. Tsukruk and Z. Huang, Polymer **41**, 5541 (2000).
[23] V. V. Tsukruk, A. Sidorenko, V. V. Gorbunov, and S. A. Chizhik, Langmuir **17**, 6715 (2001).
[24] S. A. Chizhik, Z. Huang, V. V. Gorbunov, N. K. Myshkin, and V. V. Tsukruk, Langmuir **14**, 2606 (1998).
[25] V. V. Tsukruk and V. V. Gorbunov, Microsc. Today **1**, 8 (2001).
[26] K. L. Johnson, K. Kendall, and A. D. Roberts, Proc. R. Soc. London, Ser. A **324**, 301 (1971).
[27] G. M. Phart, W. C. Oliver, and F. B. Brotzen, J. Mater. Res. **7**, 613 (1992).
[28] M. R. Vanlandingham, S. H. McKnight, G. R. Palmese, J. R. Ellings, X. Huang, T. A. Bogetti, R. F. Eduljee, and J. W. Gillespie, Adhesion **64**, 31 (1997).
[29] J. L. Hazel and V. V. Tsukruk, Thin Solid Films **339**, 249 (1999).
[30] W. J. Orts, J. H. van Zanten, and S. K. Satija, Phys. Rev. Lett. **71**, 867 (1993); T. Kajiama, K. Tanaka, and A. Takahara, Macromolecules **28**, 3482 (1995).